Metamaterial Huygens' Surfaces: Tailoring Wave Fronts with Reflectionless Sheets

Carl Pfeiffer and Anthony Grbic*

Department of Electrical Engineering and Computer Science, University of Michigan, Ann Arbor, Michigan 48109-2122, USA

(Received 10 December 2012; published 6 May 2013)

Huygens' principle is a well-known concept in electromagnetics that dates back to 1690. Here, it is applied to develop designer surfaces that provide extreme control of electromagnetic wave fronts across electrically thin layers. These reflectionless surfaces, referred to as metamaterial Huygens' surfaces, provide new beam shaping, steering, and focusing capabilities. The metamaterial Huygens' surfaces are realized with two-dimensional arrays of polarizable particles that provide both electric and magnetic polarization currents to generate prescribed wave fronts. A straightforward design methodology is demonstrated and applied to develop a beam-refracting surface and a Gaussian-to-Bessel beam transformer. Metamaterial Huygens' surfaces could find a wide range of applications over the entire electromagnetic spectrum including single-surface lenses, polarization controlling devices, stealth technologies, and perfect absorbers.

DOI: 10.1103/PhysRevLett.110.197401 PACS numbers: 78.67.Pt, 81.05.Xj

In recent years, it has been shown that extreme control of electromagnetic fields can be achieved with metamaterials. Progress in metamaterials has led to a myriad of devices ranging from perfect lenses to invisibility cloaks [1–3]. However, the notable thickness of this new class of materials often leads to significant losses as well as fabrication challenges. Therefore, reducing the thickness of these three-dimensional materials to that of a surface is highly desired. This aim has led to the development of metasurfaces: the two-dimensional equivalent of metamaterials [4]. Metasurfaces are composed of two-dimensional arrays of polarizable particles. To date, most metasurfaces have been periodic, which has generally limited their application to filters, waveguides, and absorbers [4–9]. Here, we introduce nonperiodic metasurfaces that react to both electric and magnetic fields. We will refer to these surfaces as metamaterial Huygens' surfaces, since their design is based on a rigorous formulation of Huygens' principle.

Huygens' principle qualitatively states that each point on a wave front acts as a secondary source of outgoing waves [10]. In 1901, Love developed a rigorous form of Huygens' principle, which specified the secondary sources in terms of well-defined fictitious electric and magnetic currents [11]. Schelkunoff later extended Love's equivalence principle to allow for arbitrary field distributions on either side of a surface [12]. Schelkunoff's formulation is known today as simply the surface equivalence principle, and is readily employed in the analysis of aperture antennas, diffraction problems, and computational electromagnetics formulations.

The contribution of this Letter is twofold. First, it is shown how the surface equivalence principle can be employed to design electrically thin layers (sheets) capable of establishing arbitrary field patters for a given illumination. The previously fictitious currents introduced by Schelkunoff are replaced with physical, polarization currents produced by a nonperiodic distribution of polarizable particles exhibiting both electric and magnetic responses. Secondly, it is detailed how to realize these arbitrary electric and magnetic polarization currents with metamaterial (subwavelength textured) surfaces. To outline the design methodology, a reflectionless Huygens' surface that provides a spatially varying phase response is experimentally demonstrated at microwave frequencies. This structure can be envisaged as a nonperiodic distribution of Huygens' sources [13,14].

In the surface equivalence principle, independent field distributions are stipulated in two regions of space (regions I and II of Fig. 1). Since the fields are generally discontinuous at the surface S, fictitious electric and magnetic surface currents are needed on the surface to satisfy the boundary conditions,

$$\vec{J}_s = \hat{n} \times (\vec{H}_2 - \vec{H}_1), \qquad \vec{M}_s = -\hat{n} \times (\vec{E}_2 - \vec{E}_1). \quad (1)$$

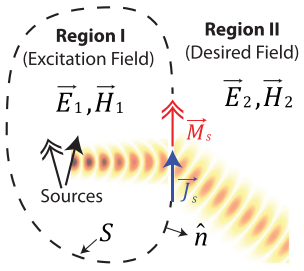

FIG. 1 (color online). Arbitrary fields in two regions separated by a closed surface S that provides electric and magnetic surface currents. The fields in regions I and II are defined independently of each other, and the surface equivalence principle is employed to find the fictitious electric and magnetic surface currents that satisfy the boundary conditions.

Here, we replace Schelkunoff's fictitious surface currents with physical, polarization currents. The polarization currents are generated by exciting a prescribed two-dimensional array of polarizable particles with an incident field. Each polarizable particle can be characterized by its quasistatic electric and magnetic polarizabilities ($\alpha_{e,m}$) defined as the ratio of the dipole moment to the local field. When these particles are closely spaced across a two-dimensional surface, a surface polarizability ($\alpha_{e,m}^{\text{eff}}$) that accounts for coupling between particles can be defined. By averaging the fields of the electric and magnetic dipole moments over S, the surface polarizability can be related to the equivalent electric and magnetic surface currents [15],

$$\vec{J}_s = j\omega\bar{\bar{\alpha}}_e^{\text{eff}} \cdot \vec{E}_{t,\text{av}}|_S, \qquad \vec{M}_s = j\omega\bar{\bar{\alpha}}_m^{\text{eff}} \cdot \vec{H}_{t,\text{av}}|_S. \quad (2)$$

A time-harmonic progression of $e^{j\omega t}$ is assumed, where ω is the radial frequency and t is the time. The expressions $\vec{E}_{t,\text{av}}|_S$ and $\vec{H}_{t,\text{av}}|_S$ represent the average electric and magnetic fields tangential to the surface S.

The surface equivalence principle is generally formulated in terms of fields and surface currents at a boundary. Therefore it may be more appropriate to define an impedance boundary condition. This can be done by defining an electric sheet admittance ($\bar{\bar{Y}}_{\text{es}} = j\omega\bar{\bar{\alpha}}_e^{\text{eff}}$) and magnetic sheet impedance ($\bar{\bar{Z}}_{\text{ms}} = j\omega\bar{\bar{\alpha}}_m^{\text{eff}}$) in terms of the surface polarizabilities. In general, $\bar{\bar{Y}}_{\text{es}}$ and $\bar{\bar{Z}}_{\text{ms}}$ are tensorial quantities. For illustration purposes, we will assume that the sheet impedance is isotropic: $Y_{\text{es}} = Y_{\text{es}}^{yy} = Y_{\text{es}}^{zz}$ and $Z_{\text{ms}} = Z_{\text{ms}}^{yy} = Z_{\text{ms}}^{zz}$ for a sheet in the $x = 0$ plane.

Once the necessary values of Y_{es} and Z_{ms} are known, the surface is discretized into unit cells. The surface impedance of each cell is then realized through subwavelength texturing of a metallic cladding on a dielectric substrate. Field averaging techniques could be employed to find $\alpha_{e,m}^{\text{eff}}$ for a designed metallic pattern [15], but a more straightforward method is used here. The impedance is directly extracted from the complex reflection (R) and transmission (T) coefficients. As demonstrated in [16], R and T can be related to the sheet impedances of a periodic metasurface for a normally incident plane wave,

$$Y_{\text{es}} = \frac{2(1 - T - R)}{\eta(1 + T + R)}, \qquad Z_{\text{ms}} = \frac{2\eta(1 - T + R)}{(1 + T - R)}, \quad (3)$$

where $\eta = \sqrt{\mu/\epsilon}$ is the wave impedance of free space. From Eq. (3), it can be easily shown that if the normalized electric sheet admittance and magnetic sheet impedance are equal and purely imaginary ($Y_{\text{es}}\eta = Z_{\text{ms}}/\eta$), the amplitude of the unit cell's transmission coefficient becomes unity. In addition, the transmitted phase can be varied anywhere between $-180°$ and $+180°$ to provide complete phase coverage by adjusting the magnitude of the impedance.

Metamaterial Huygens' surfaces introduce abrupt field discontinuities across electrically thin layers. They are distinct from the work of Nanfang Yu *et al.* [17,18] and Xingjie Ni *et al.* [19], which also allow field discontinuities. Unlike the metamaterial interfaces reported by these two groups, Huygens' surfaces do not incur reflection losses and are not restricted to solely manipulating the phase of cross-polarized radiation. Huygen's surfaces can fully manipulate both copolarized and cross-polarized radiation. This polarization control can be used to generate linear, circular, or elliptical polarization from a given excitation without reflection. Finally, Huygens' surfaces can redirect an incident beam with nearly 100% efficiency into a refracted beam. This is in contrast to the metamaterial interfaces reported earlier, which necessarily incurred reflection due to their exclusively electric response and produced two refracted beams: an ordinary beam in addition to the anomalous beam. An alternative method that efficiently manipulates a wave front involves stacking multiple layers of frequency selective surfaces [20–24]. However, a typical structure requires seven layers to realize full 360° phase coverage. This presents added fabrication and design challenges.

In this work, a metamaterial Huygens' surface was developed to efficiently refract a normally incident plane wave to an angle $\phi = 45°$ from normal, as shown in Fig. 2(a).

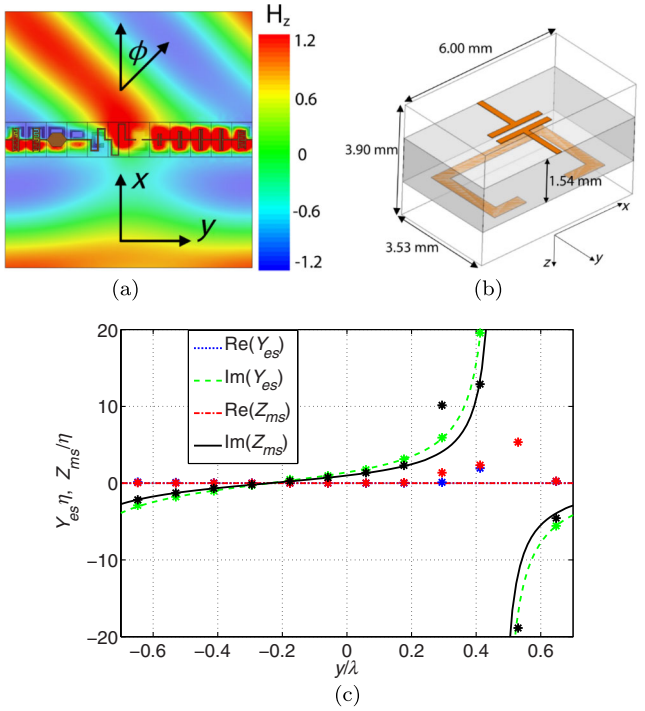

FIG. 2 (color online). (a) Simulated time snapshot of the magnetic field (H_z) of a $\hat{y}$-polarized plane wave, normally incident upon the designed Huygens' surface. (b) Dimensions of the unit cells comprising the metamaterial Huygens' surface. The particular unit cell shown has $Y_{\text{es}} = (0.02 + 3.14j)/\eta$ and $Z_{\text{ms}} = (0.07 + 2.3j)\eta$. (c) One period of the real and imaginary sheet impedances to refract a normally incident electromagnetic wave to an angle of 45°. Lines are the computed values, and asterisks are the simulated values.

The fields are TM-polarized (magnetic field is $\hat{z}$-polarized), and an operating frequency of 10 GHz was chosen. Once the fields in regions I and II are stipulated, the necessary sheet impedances can be found straightforwardly. The design details for this specific example are described in the Supplemental Material [25].

Since the incident and refracted waves are plane waves, the sheet impedances exhibit periodicity in the $\hat{y}$ direction with a period of $\lambda/\sin(\phi)$. Each period is discretized into 12 unit cells consisting of patterned copper traces on a low loss, Roger's RO4003 substrate [$\epsilon_r = 3.55$, $\tan(\delta) = 0.0027$]. The top layer of the substrate presents capacitively and inductively loaded traces to realize both positive and negative electric sheet reactances. The bottom layer presents capacitively loaded loops (split-ring resonators) to realize the magnetic sheet reactances [26]. The sheet impedances extracted from simulation along with the desired values are plotted in Fig. 2(c). In Fig. 2(b), a unit cell with $Y_{\text{es}} = (0.02 + 3.14j)/\eta$ and $Z_{\text{ms}} = (0.07 + 2.3j)\eta$ is shown. The designed Huygens' surface was then simulated using a commercial full-wave electromagnetics solver (Ansoft HFSS). Figure 2(a) shows a steady-state time snapshot of the simulated $\hat{z}$-directed magnetic field. The plane wave normally incident from the bottom is steered to $\phi = 45°$ by the metamaterial Huygens' surface. From simulation, 4.7% of the incident power is absorbed by the Huygens' surface and 3.9% is scattered into undesired directions. In addition, the Huygens' surface maintains a relatively constant performance when the angle of the incident wave is scanned over a range of 80°. A more in-depth discussion of the efficiency and angular dependence is provided in the Supplemental Material [25].

To experimentally measure the performance of the metamaterial Huygens' surface, the normally incident plane wave was approximated with a Gaussian beam with a 57 mm beam waist [25]. This required the fabricated surface to be 226 mm × 226 mm to capture 99.9% of the incident power [27]. A section of the fabricated Huygens' surface is shown in Fig. 3(a). It is composed of a vertical stack of 58 identical circuit board strips, with 2.35 mm air gaps between each of the boards. The top and bottom sides of the boards are shown in Figs. 3(b) and 3(c), which provide the required electric and magnetic polarization currents, respectively. The Huygens' surface was measured using a near field scanning system [25,28], and the performance is summarized in Figs. 4(a)–4(e) [25]. All the contour plots of Figs. 4(a)–4(d) are normalized by the magnitude of the incident Gaussian beam. The ratio of power transmitted in the refracted direction to the incident power over the operating frequencies is plotted in Fig. 4(e). The half-powered bandwidth and peak efficiency of the structure were measured to be 24.2% and 86%, respectively.

Next, a metamaterial Huygens' surface that provides beam shaping capabilities is demonstrated with a Gaussian-to-Bessel beam transformer [18,25]. This

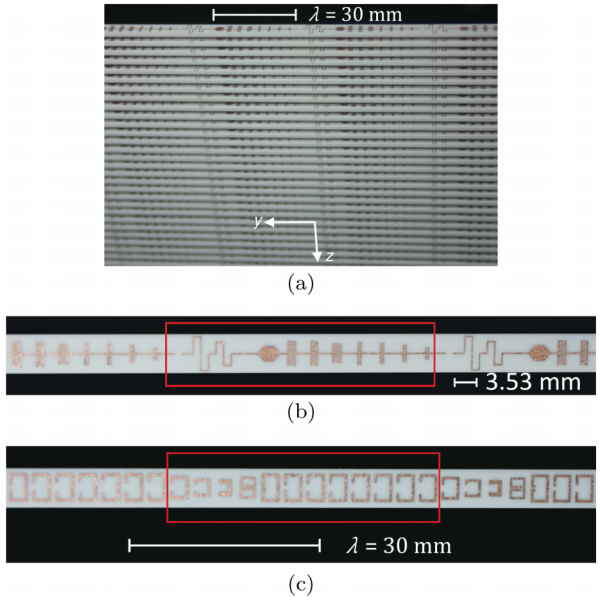

FIG. 3 (color online). (a) Photograph of the fabricated Huygens' surface. (b) Copper traces on the top side of each substrate provide the necessary electric polarization currents. The pattern inside the red box repeats itself every 12 unit cells. (c) Split-ring resonators on the bottom side of each substrate provide the necessary magnetic polarization currents.

example is particularly interesting because Bessel beams confine their energy to a narrow beamwidth, which has applications in fields such as near field probing, medical imaging, and radiometry [29,30]. For simplicity, we assume the fields are invariant along $\hat{z}$, and the electric field is $\hat{z}$-polarized. Since ideal Bessel beams carry infinite energy, they must be truncated with a windowing function (a Gaussian was chosen), which causes them to diffract. To compensate for this, the field just behind the Huygens' surface in region II is stipulated to be the phase conjugated wave front of a diffracted Bessel beam. This causes the wave front to refocus to the desired Bessel beam profile at the designed focal plane ($x = 8.33\lambda$). Once the fields at the Huygens' surface are specified, the necessary reactive sheet impedances are determined. In simulation, the computed impedances are realized with electrically thin (in terms of free space wavelengths) material slabs with identical reflection and transmission coefficients as the desired sheet impedance. This permits the use of commercial electromagnetic solvers for simulation, while maintaining virtually identical performance. Figure 5(a) shows the magnitude of the simulated $\hat{z}$-directed electric field. The Gaussian beam at $x < 0$ is transformed into a Bessel beam at $x > 0$ with greater than 99% transmission. In Fig. 5(b) the simulated and desired values of $|E_z|$ are plotted at the input face of the Huygens' surface ($x = -1.67\lambda$) and at the focal plane ($x = 8.33\lambda$).

The developed metamaterial Huygens' surfaces use both electric and magnetic polarization currents to manipulate

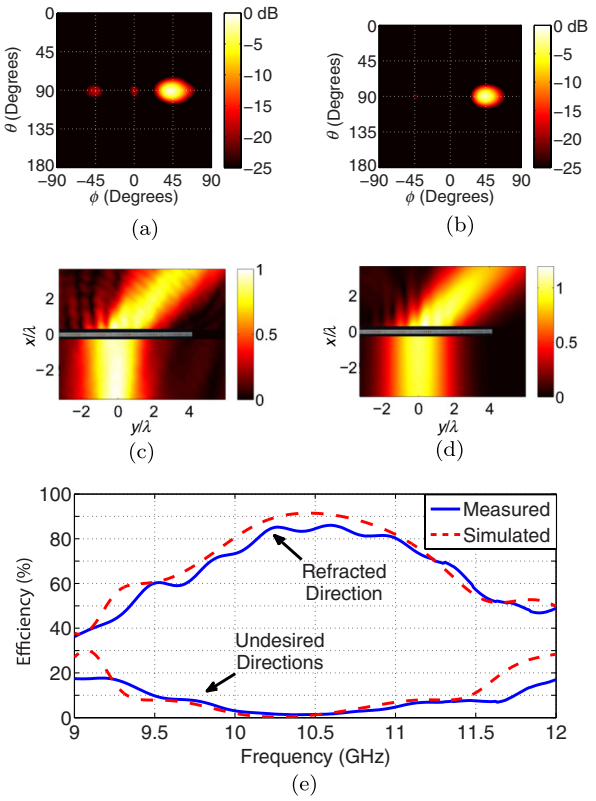

FIG. 4 (color online). (a and b) Measured and simulated far field radiation patterns, respectively. (c and d) Measured and simulated magnetic field magnitudes in the xy plane, respectively. The incident field is shown for $x < 0$, and the transmitted field is shown for $x > 0$. (e) Measured and simulated efficiency of the Huygens' surface. The efficiency is defined as the ratio of the power in the refracted beam to the incident power.

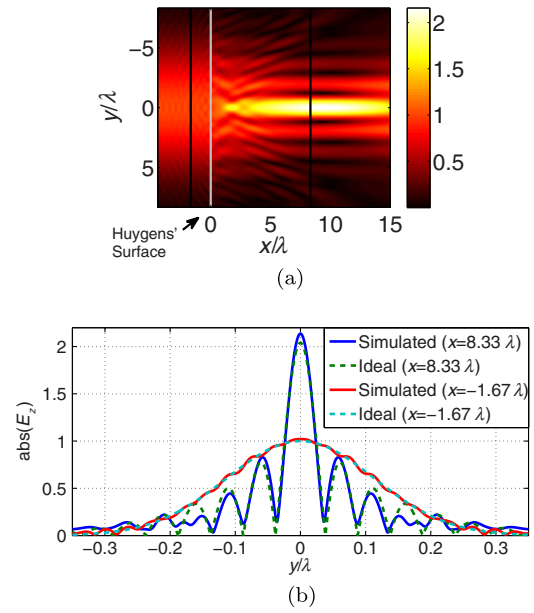

FIG. 5 (color online). (a) Electric field (E_z) magnitude of a two-dimensional Gaussian beam incident upon a Gaussian-to-Bessel beam transformer located at $x = 0$. (b) Simulated and computed electric field magnitude at the focal plane ($x = 8.33\lambda$) and at the input face of the Huygens's surface ($x = -1.67\lambda$).

electromagnetic wave fronts without reflection. These surfaces are composed of electrically small, polarizable particles which provide surface currents that satisfy the surface equivalence principle between two regions. A design methodology was developed and applied to demonstrate beam steering and shaping. A proof-of-concept Huygens' surface was experimentally demonstrated at microwave frequencies.

Metamaterial Huygens' surfaces could enable a myriad of novel devices. Surfaces possessing tensorial electric sheet admittances and magnetic sheet impedances with off-diagonal entries could enable devices that manipulate the field profile and allow polarization control such as linear-to-circular polarization conversion [31]. Further, nonperiodic metasurfaces of bianisotropic particles could allow arbitrary polarization control and beam shaping. Such surfaces would build on recent work showing that periodic metasurfaces exhibiting bianisotropy can perform any plane-wave polarization transformation [32]. Huygens' surfaces may also find use in stealth applications. For example, two-dimensional arrays of electric and magnetic polarizable particles could be used to tailor reflected wave fronts. In addition, absorbers that are impedance matched to nonuniform wave fronts could be designed [33]. Finally, metamaterial Huygens' surfaces could be extended to optical frequencies with the inclusion of plasmonic and dielectric polarizable particles [34,35].

This work was supported by a Presidential Early Career Award for Scientists and Engineers (Grant No. FA9550-09-1-0696) and the National Science Foundation Materials Research Science and Engineering Center program DMR Grant No. 1120923 (Center for Photonics and Multiscale Nanomaterials at the University of Michigan).

*Corresponding author.
agrbic@umich.edu

[1] D. Smith, J. Pendry, and M. Wiltshire, Science **305**, 788 (2004).
[2] J. Pendry, D. Schurig, and D. Smith, Science **312**, 1780 (2006).
[3] D. Schurig, J. Mock, B. Justice, S. Cummer, J. Pendry, A. Starr, and D. Smith, Science **314**, 977 (2006).
[4] C. L. Holloway, E. R. Kuester, J. A. Gordon, J. O'Hara, J. C. Booth, and D. R. Smith, IEEE Trans. Antennas Propag. **54**, 10 (2012).
[5] C. L. Holloway, E. R. Kuester, and D. R. Novotny, IEEE Trans. Antennas Wireless Propag. Lett. **8**, 525 (2009).
[6] J. A. Gordon, C. L. Holloway, and A. Dienstfrey, IEEE Trans. Antennas Wireless Propag. Lett. **8**, 1127 (2009).
[7] C. Fietz and G. Shvets, Phys. Rev. B **82**, 205128 (2010).

[8] S. Tretyakov, *Analytical Modeling in Applied Electromagnetics* (Artech House, Inc., Norwood, MA, 2003).
[9] Y. Avitzour, Y. A. Urzhumov, and G. Shvets, Phys. Rev. B **79**, 045131 (2009).
[10] C. Huygens, *Traité de la Lumière* (Pieter van der Aa, Leyden, 1690).
[11] A. Love, Philos. Trans. R. Soc. A **197**, 1 (1901).
[12] S. Schelkunoff, Bell Syst. Tech. J. **15**, 92 (1936).
[13] P. Jin and R. W. Ziolkowski, IEEE Trans. Antennas Wireless Propag. Lett. **9**, 501 (2010).
[14] A. Karilainen and S. Tretyakov, IEEE Trans. Antennas Propag. **60**, 3471 (2012).
[15] E. Kuester, M. Mohamed, M. Piket-May, and C. Holloway, IEEE Trans. Antennas Propag. **51**, 2641 (2003).
[16] C. Holloway, M. Mohamed, E. Kuester, and A. Dienstfrey, IEEE Transactions on Electromagnetic Compatibility **47**, 853 (2005).
[17] N. Yu, P. Genevet, M. Kats, F. Aieta, J. Tetienne, F. Capasso, and Z. Gaburro, Science **334**, 333 (2011).
[18] F. Aieta, P. Genevet, M. A. Kats, N. Yu, R. Blanchard, Z. Gaburro, and F. Capasso, Nano Lett. **12**, 4932 (2012).
[19] X. Ni, N. Emani, A. Kildishev, A. Boltasseva, and V. Shalaev, Science **335**, 427 (2012).
[20] M. Al-Joumayly and N. Behdad, IEEE Trans. Antennas Propag. **58**, 4033 (2010).
[21] D. Pozar, Electron. Lett. **32**, 2109 (1996).
[22] K. Sarabandi and N. Behdad, IEEE Trans. Antennas Propag. **55**, 1239 (2007).
[23] C. Ryan, M. Chaharmir, J. Shaker, J. Bray, Y. Antar, and A. Ittipiboon, IEEE Trans. Antennas Propag. **58**, 1486 (2010).
[24] B. Memarzadeh and H. Mosallaei, Opt. Lett. **36**, 2569 (2011).
[25] See Supplemental Material at http://link.aps.org/supplemental/10.1103/PhysRevLett.110.197401 for additional information on the measurement and design of a beam-refracting Huygens' surface.
[26] D. R. Smith, W. J. Padilla, D. C. Vier, S. C. Nemat-Nasser, and S. Schultz, Phys. Rev. Lett. **84**, 4184 (2000).
[27] P. Goldsmith, Proc. IEEE **80**, 1729 (1992).
[28] A. Yaghjian, IEEE Trans. Antennas Propag. **34**, 30 (1986).
[29] J. Durnin, J. J. Miceli, and J. H. Eberly, Phys. Rev. Lett. **58**, 1499 (1987).
[30] D. McGloin and K. Dholakia, Contemp. Phys. **46**, 15 (2005).
[31] N. Yu, F. Aieta, P. Genevet, M. A. Kats, Z. Gaburro, and F. Capasso, Nano Lett. **12**, 6328 (2012).
[32] T. Niemi, A. O. Karilainen, and S. A. Tretyakov, in *Proceedings of the IEEE Antennas and Propagation Society International Symposium (APSURSI)* (IEEE, Chicago, IL, 2012), pp. 1–2.
[33] R. Alaee, C. Menzel, C. Rockstuhl, and F. Lederer, Opt. Express **20**, 18370 (2012).
[34] V. Shalaev, Nat. Photonics **1**, 41 (2007).
[35] N. Engheta, A. Salandrino, and A. Alù, Phys. Rev. Lett. **95**, 095504 (2005).